THE PARAMETRIZATION OF SUB-GRID SCALE OROGRAPHY

S.D. Mobbs
University of Leeds
Leeds LS2 9JT, U.K.

Summary: The theory of internal gravity waves is reviewed with particular emphasis on properties which are relevant to the problem of parametrization of wave-induced drag in numerical models. Observational techniques for gravity wave study are also described. Finally, a simplified account of a gravity wave drag parametrization scheme is given.

1. INTRODUCTION

It is now well-known that momentum transport associated with sub-grid scale orographic effects needs to be included in numerical weather prediction models in order that they should reproduce observed climatologies. Evidence for this is presented, for example, by Palmer *et al.* (1986). It is further recognised that the principal process involved in the vertical transport of momentum on sub-grid scales (i.e. less than a few hundred kilometres) is that of orographic gravity wave propagation. This paper describes the major physical processes involved in the generation, propagation and dissipation of orographic gravity waves and relates them to simple parametrizations of the sub-grid scale momentum transport. Sections 2-10 are concerned gravity wave theory. Sections 11 and 12 deal with observational techniques and in section 13 a simple gravity wave drag parametrization scheme is described.

2. LINEAR INTERNAL GRAVITY WAVES

We consider linear internal gravity waves with zero phase speed (appropriate for orographic waves) and horizontal wavevector $\boldsymbol{\kappa} = (k, \ell)$. The vertical velocity in a field of such waves may be represented by a Fourier superposition of modes:

$$w(x,y,z) = \int_{-\infty}^{\infty}\int_{-\infty}^{\infty} \widehat{w}(k,\ell,z) e^{i(kx+\ell y)}\,\mathrm{d}k\mathrm{d}\ell. \tag{1}$$

It is readily shown that $\widehat{w}$ satisfies the vertical structure (Taylor-Goldstein) equation:

$$\frac{\mathrm{d}^2\widehat{w}}{\mathrm{d}z^2} + \left[\frac{N^2(k^2+\ell^2)}{(Uk+V\ell)^2} - \frac{U''k+V''\ell}{Uk+V\ell} - (k^2+\ell^2)\right]\widehat{w} = 0 \tag{2}$$

where N is the Brunt-Väisälä frequency and $\boldsymbol{U} = (U(z), V(z))$ is the mean flow velocity. Consider a simple mean flow which is independent of height. We can always take $V = 0$ by an appropriate rotation of coordinates. If we look for a solution which is wave-like in the vertical, i.e.

$$\widehat{w} \sim e^{imz}, \tag{3}$$

then

$$k^2 + m^2 = \frac{N^2}{U^2}. \tag{4}$$

It follows that if m is real (i.e. the flow is wave-like in the vertical) then the horizontal wavelength λ_x must satisfy the condition

$$\lambda_x = \frac{2\pi}{k} > \frac{2\pi U}{N}. \tag{5}$$

If the horizontal wavelength is less than this value, then m is imaginary and the wave amplitude decays exponentially with height.

It is the wave-like modes, with wavelengths greater than $2\pi U/N$ which are associated with orographic drag. The critical wavelength $2\pi U/N$ is usually a few kilometres and is therefore not resolved by numerical weather prediction models (except for some regional models).

3. OROGRAPHIC STRESS

Orographic stress is the force per unit horizontal area exerted on the atmosphere by orography. Fundamental processes are:

(a) stratification;

(b) turbulence (on boundary layer scale);

(c) rotation (on large scales).

Here we are concerned primarily with the orographic stress caused by the generation of internal gravity waves and we are therefore concerned mainly with the effects of stratification.

The essential mechanism of internal gravity wave drag may be illustrated by the example of two-dimensional, wavy orography (Fig. (1)).

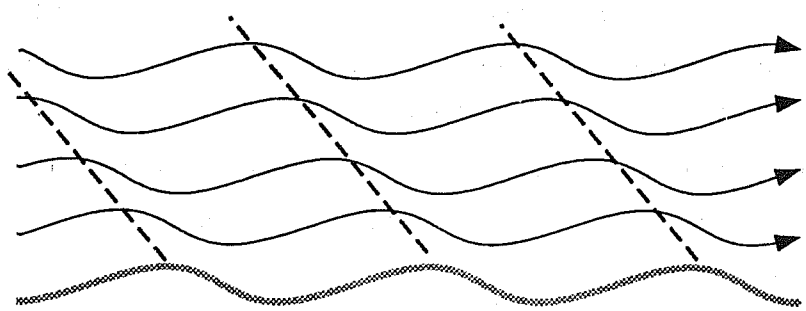

Fig. 1 Streamlines for stratified flow over "wavy" orography. If the horizontal wavelength is large enough, internal gravity waves will be generated and the phase lines will slope with height.

The slope of the lines of constant phase in Fig. (1) is the cause of the force on the orography. The Bernoulli equation for an incompressible flow (a good enough approximation here) is

$$\frac{U^2}{2} + \frac{p}{\rho_0} + gz = \text{constant on streamlines.} \tag{6}$$

This equation indicates that regions of high velocity will be associated with low pressure and *vice versa*. Fig. (2) shows the pressure pattern associated with the streamlines shown in Fig. (1). This allows us to examine the pressure force on any layer of fluid lying between two streamlines (see Fig (3)). It is evident from the figure that the forces on the upper and lower sides of the layer are of opposite sign and if the wave-field does not change in amplitude with height, it seems likely that the resultant force is zero. We shall see later that this is indeed the case.

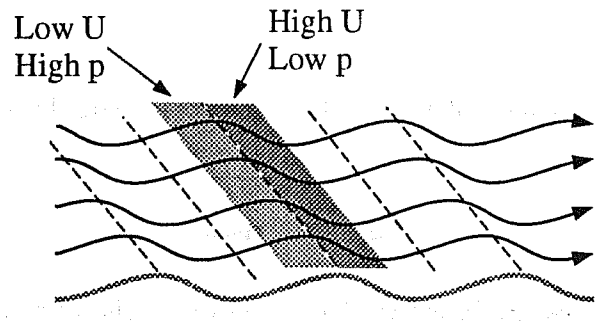

Fig. 2 Regions of high and low pressure in a wave field, according to Bernoulli's equation.

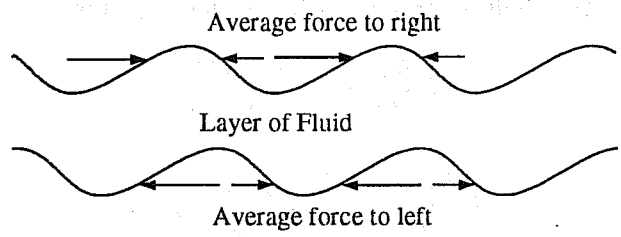

Fig. 3 The external horizontal pressure forces on a layer of fluid lying between two streamlines.

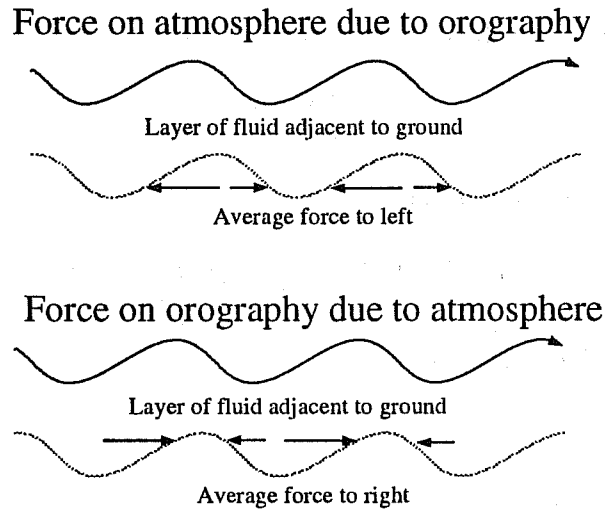

Fig. 4 The pressure force on the atmosphere due to the orography (the orographic stress) and the pressure force on the orography due to the atmosphere.

If we now examine the layer of air in contact with the wavy ground, we can see both the effect of the orography on the atmosphere as a whole and also the effect of the atmosphere on the orography

(Fig. (4)).

Of course Newton's third law relates the force on the orography ($F_{\mathbf{orog}}$) to the force on the atmosphere ($F_{\mathbf{atmos}}$):

$$F_{\mathbf{orog}} = -F_{\mathbf{atmos}}. \tag{7}$$

This means that, although we are interested in the force on the atmosphere, we can, if we wish, measure the force on the orography (see §11).

4. INTERNAL GRAVITY WAVE STRESS

The way in which internal gravity waves transmit stress may be illustrated using two dimensional, shallow Boussinesq theory. We shall neglect mean wind shear for now.

$$U\frac{\partial u'}{\partial x} = -\frac{\partial}{\partial x}\left(\frac{p'}{\rho_0}\right); \tag{8}$$

$$U\frac{\partial w'}{\partial x} = -\frac{\partial}{\partial z}\left(\frac{p'}{\rho_0}\right) - g\frac{\rho'}{\rho_0}; \tag{9}$$

$$U\frac{\partial}{\partial x}\left(\frac{\rho'}{\rho_0}\right) + \frac{1}{\rho_0}\frac{\mathrm{d}\rho_0}{\mathrm{d}z}w' = 0; \tag{10}$$

$$\frac{\partial u'}{\partial x} + \frac{\partial w'}{\partial z} = 0. \tag{11}$$

We also need the vertical displacement of fluid elements, ζ:

$$U\frac{\partial \zeta}{\partial x} = w'. \tag{12}$$

By assuming a steady plane wave solution:

$$\left[u',\, w',\, \frac{p'}{\rho_0},\, \frac{\rho'}{\rho_0}\right] = \left[\widehat{u},\, \widehat{w},\, \widehat{P},\, \widehat{R}\right] e^{i(kx+mz)}, \tag{13}$$

we obtain the so-called "polarisation relations":

$$ikU\widehat{u} = -ik\widehat{P}; \tag{14}$$

$$ikU\widehat{w} = -im\widehat{P} - g\widehat{R}; \tag{15}$$

$$ikU\widehat{R} + \frac{1}{\rho_0}\frac{\mathrm{d}\rho_0}{\mathrm{d}z}\widehat{w} = 0; \tag{16}$$

$$ik\widehat{u} + im\widehat{w} = 0. \tag{17}$$

The horizontal force per unit area on a wavy surface can be found as shown in Fig. (5).

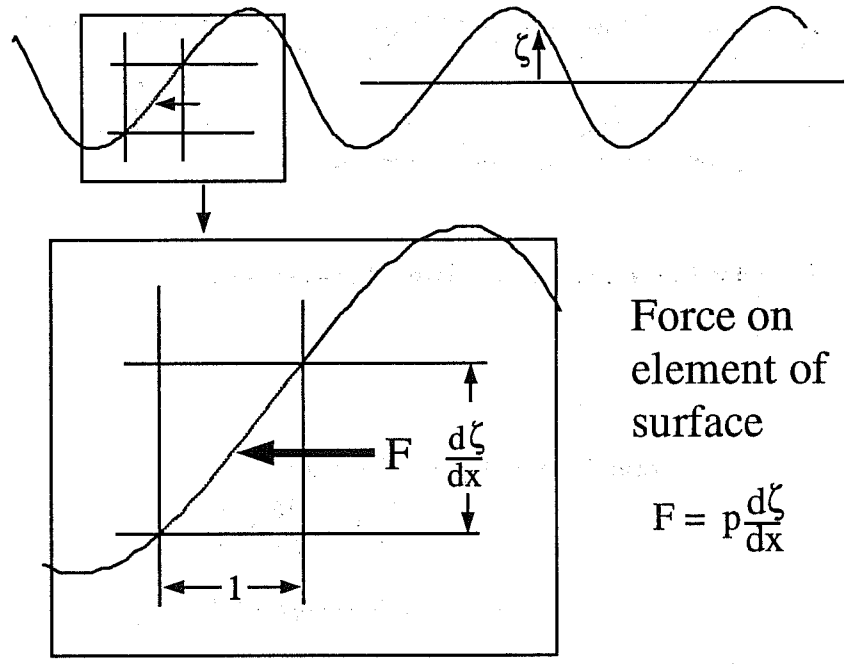

Fig. 5 Horizontal pressure force on a material surface deformed by internal gravity waves.

From Fig. (5) we can see that

$$\text{Horizontal force per unit area} = p\frac{\partial \zeta}{\partial x}. \tag{18}$$

Averaging horizontally over a wavelength we get:

$$\text{Average horizontal force per unit area} = \overline{p'\frac{\partial \zeta}{\partial x}}. \tag{19}$$

But

$$\frac{\partial \zeta}{\partial x} = \frac{w'}{U} \tag{20}$$

and from the polarization relation

$$p' = -\rho_0 U u'. \tag{21}$$

Hence

$$\text{Average horizontal force per unit area} = F = -\rho_0 \overline{u'w'}. \tag{22}$$

In order to see how this affects a thin layer of fluid between material surfaces, consider Fig. (6).

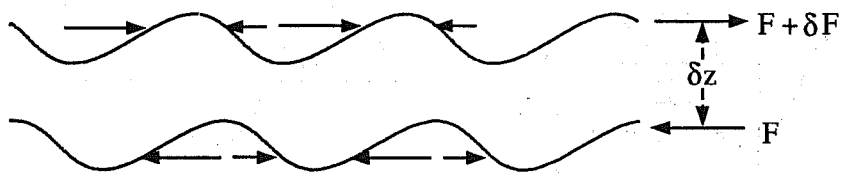

Fig. 6 Resultant force due to wave stress on a layer of thickness δz.

$$\begin{aligned}\text{Total force on layer} &= (F+\delta F) - F \\ &= \left(F + \frac{\partial F}{\partial z}\delta z\right) - F \\ &= -\frac{\partial}{\partial z}(\rho_0 \overline{u'w'})\delta z \end{aligned} \tag{23}$$

The mass of layer per unit area is $\rho_0 \delta z$ and so the horizontal equation of motion of the layer is

$$\rho_0 \frac{\partial \overline{u}}{\partial t} = -\frac{\partial}{\partial z}(\rho_0 \overline{u'w'}). \tag{24}$$

Hence the resultant force is only non-zero when $\rho_0 \overline{u'w'}$ changes with height. $\rho_0 \overline{u'w'}$ is the wave-induced vertical flux of horizontal momentum.

Gravity wave parametrization is fundamentally concerned with representing the change with height of $\rho_0 \overline{u'w'}$ (or more generally the vector $(\rho_0 \overline{u'w'}, \rho_0 \overline{v'w'})$, where the prime denotes sub-grid scale gravity wave motion.

5. THE ELIASSEN-PALM THEOREM

Before considering how to represent the height variation of the wave-induced flux of horizontal momentum in large scale models, it is useful to consider any fundamental dynamical constraints which this quantity is likely to obey. The most important such constraint is expressed by the Eliassen-Palm theorem (Eliassen and Palm 1961). This can be stated as follows:

> *For a steady wave field in the absence of dissipation, the vertical flux of horizontal momentum $\rho_0 \overline{u'w'}$ is independent of height except at levels where the mean wind U is zero (critical levels).*

A derivation of the Eliassen-Palm theorem is given in the appendix. The consequence of the Eliassen-Palm theorem is that the wave stress only causes a non-zero force on the atmosphere near critical levels or where dissipative processes act.

We can now illustrate a conceptual idea of how and where wave-induced mean forces are likely to act on the atmosphere (see Fig. (7)).

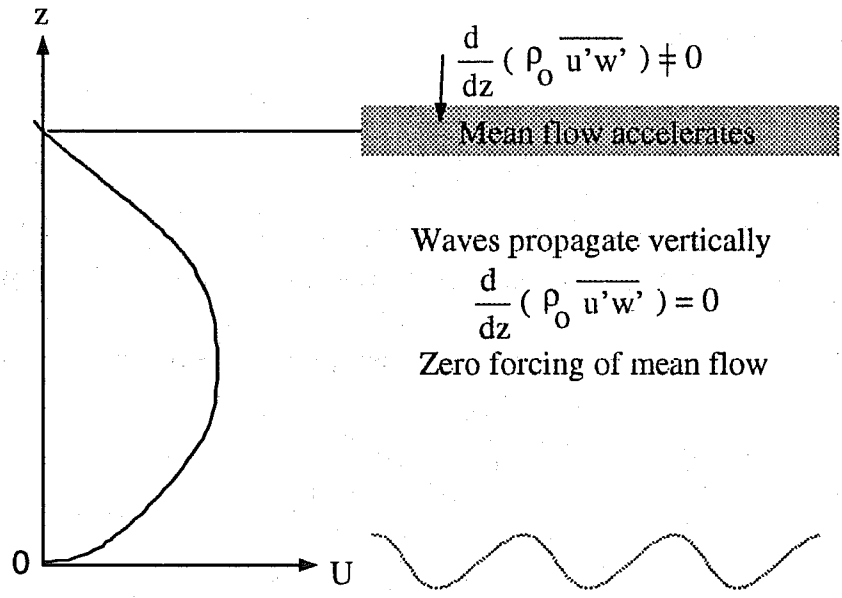

Fig. 7 The overall picture showing where there is likely to be a wave induced mean force (drag) on the atmosphere.

6. WAVE BREAKING AND SATURATION

It is shown in the appendix that the vertical flux of wave energy is not constant with height when there is a mean shear. This is just one reason for the wave amplitude varying with height. Another reason is the so-called "density effect". Both of these processes can be illustrated by a useful property of waves: the conservation of wave action. Neglecting dissipation, this may be expressed to a good approximation by the Bretherton and Garrett equation (Bretherton and Garrett 1968):

$$\frac{\partial}{\partial t}\left(\frac{E}{|\widehat{\omega}|}\right)+\frac{\partial}{\partial x}\left(c_{gz}\frac{E}{|\widehat{\omega}|}\right)=0. \tag{25}$$

E is the wave energy density:

$$E=\frac{1}{2}\rho_0(u'^2+w'^2)+\frac{1}{2}\rho_0 N^2\zeta^2 \tag{26},$$

c_{gz} is the vertical component of the group velocity and

$$|\widehat{\omega}|=|\omega-Uk| \tag{27}$$

is the Doppler-shifted or intrinsic frequency. For stationary waves $\omega = 0$ so $|\widehat{\omega}| = |Uk|$ and for a stationary wave field, the time derivative in Eq. (25) may be neglected. The effect of variation of U with height is described in the next section. The effect of varying density with height is qualitatively as follows. Define a scale height for density, H. Then roughly

$$\rho_0=\rho_{00}e^{-z/H}. \tag{28}$$

Since $E \propto \rho_0$ and $E \propto (u'^2 + w'^2)$, it seems plausible that since the wave action flux $c_{gz}E/|Uk|$ must be independent of height, then $u'^2, w'^2 \propto \rho_0^{-1/2}$. A full justification requires examination of the full

equations of motion and it is readily shown that

$$u',\ w',\ \theta' \propto \rho_0^{-1/2} = e^{z/2H}; \tag{29}$$

$$p' \propto \rho_0^{1/2} = e^{-z/2H}. \tag{30}$$

The density effect causes a growth of wave amplitude with height and this leads to overturning of material surfaces (Fig. (8)). This is "wave breaking". Turbulence is generated and the waves dissipate.

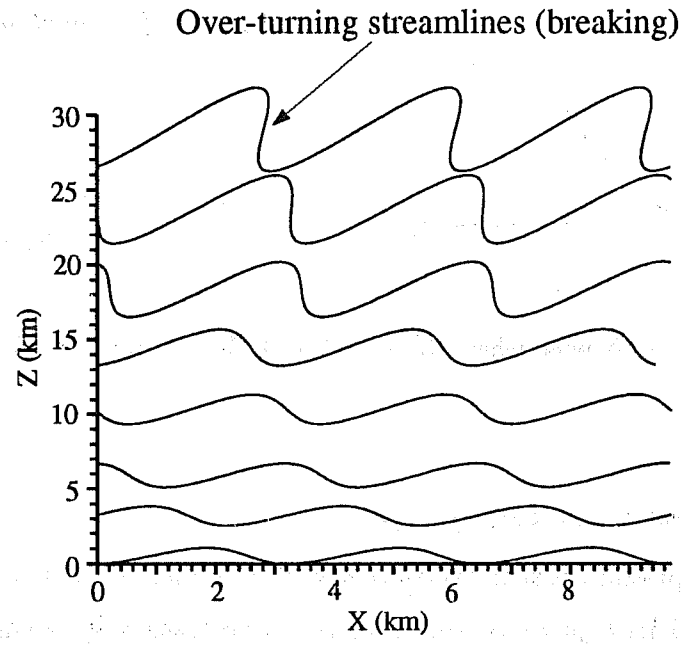

Fig. 8 Material surfaces in a wave field showing the increase in amplitude with height due to the density effect, and the consequent overturning of surfaces.

Clearly wave-breaking will reduce the amplitude of the waves. A simple model of this involves the so-called *saturation hypothesis* (e.g. Lindzen 1981). According to this idea, there is just sufficient turbulence generation to limit the wave amplitude so that material surfaces become locally vertical but do not overturn. An estimate of the wave amplitude required for saturation may be made as follows. The linearised potential temperature equation is

$$U\frac{\partial\theta'}{\partial x} + V\frac{\partial\theta'}{\partial y} + w\frac{\mathrm{d}\Theta}{\mathrm{d}z} = 0 \tag{31}$$

where $\Theta(z)$ is the mean potential temperature and θ' is the perturbation. Assuming two dimensional plane waves with y wavenumber zero, we have

$$ikU\widehat{\theta} + \widehat{w}\frac{\mathrm{d}\Theta}{\mathrm{d}z} = 0 \tag{32}$$

using the notation of §4. The vertical displacement amplitude $\widehat{\zeta}$ can be related to the vertical velocity amplitude $\widehat{w}$ using Eq. (12):

$$ikU\widehat{\zeta} = \widehat{w}. \tag{33}$$

From Eq. (32) and (33) it follows that

$$\frac{\partial\theta}{\partial z} = \frac{\mathrm{d}\Theta}{\mathrm{d}z}\left(1 - im\widehat{\zeta}e^{ikx}\right). \tag{34}$$

It is evident that overturning occurs if

$$|\widehat{\zeta}| > \frac{1}{|m|}. \tag{35}$$

7. CRITICAL LEVELS

Let us assume that the mean flow varies with height slowly so that the dispersion relation, Eq. (4) is still valid. Then

$$m = \pm\left(\frac{N^2}{U^2} - k^2\right)^{1/2}. \tag{36}$$

The group velocity for internal gravity waves can be obtained by retaining time dependence in the linearised equations of motion and looking for wave mode $\sim e^{i(kx+mz-\omega t)}$. The dispersion relation then becomes

$$\omega - Uk = \pm\frac{Nk}{(k^2+m^2)^{1/2}}. \tag{37}$$

The vertical component of the group velocity (i.e. the velocity of energy propagation) is $c_{gz} = \partial\omega/\partial m$. It follows that

$$c_{gz} = \frac{Nm}{(k^2+m^2)^{3/2}}. \tag{38}$$

We can now deduce from Eq. (36) and Eq. (38) what happens as waves approach a critical level (i.e. a level where $U = 0$):

1. $m \to \infty$. The vertical wavelength tends to zero.
2. $c_{gz} \to 0$. Wave energy takes an infinite time to arrive.

Now from the Bretherton and Garrett equation, Eq. (25), we know that for a steady field of stationary waves

$$c_{gz}\frac{E}{Uk} = \text{constant}. \tag{39}$$

From Eq. (36) and (38) it is easily shown that as $U \to 0$

$$\frac{c_{gz}}{Uk} \propto U$$

and hence

$$E \propto \frac{1}{U} \tag{40}$$

as the critical level is approached. In practice, the increase in wave amplitude causes the waves to break and dissipate. Fig. (9) shows schematically the type of wave pattern which results.

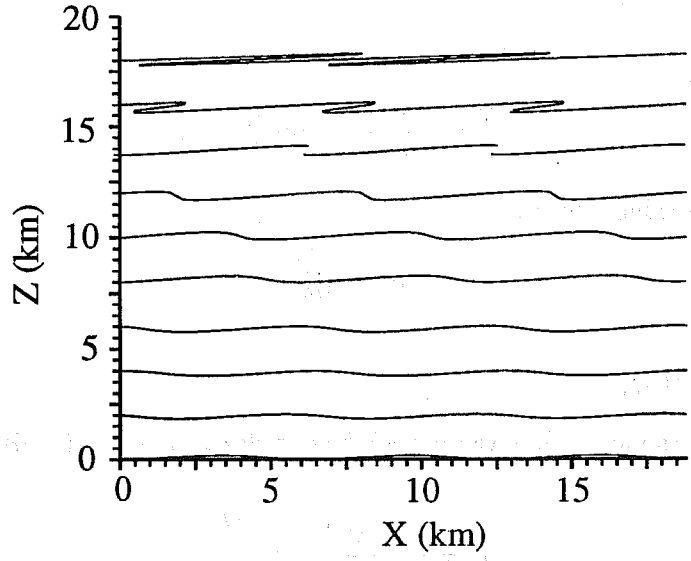

Fig. 9 Material surfaces for an internal gravity wave field approaching a critical level at 20 km. Note the severe overturning.

8. LEE WAVES AND VERTICALLY PROPAGATING WAVES

Let us return to the vertical structure equation, Eq. (2), and consider a plane wave mode with $\ell = 0$ (there is no loss of generality here because for any wave mode we can always rotate the axes to that the wave-vector is along the x-axis).

$$\frac{\mathrm{d}^2\widehat{w}}{\mathrm{d}z^2} + \left[\frac{N^2}{U^2} - \frac{U''}{U} - k^2\right]\widehat{w} = 0 \tag{41}$$

The quantity

$$\frac{N^2}{U^2} - \frac{1}{U}\frac{\mathrm{d}^2 U}{\mathrm{d}z^2} = \ell_s^2 \tag{42}$$

is called the "Scorer parameter". There are two distinct cases:

(a) $\ell_s^2 > k^2$. These are generally longer wavelength waves. There is vertical propagation, phase lines slant with height and there is a non-zero wave stress.

(b) $\ell_s^2 < k^2$. These are generally shorter wavelength waves. There is no vertical propagation. Phase lines are vertical and the amplitude decays exponentially with height. There is zero wave stress.

Lee waves are a special case of $\ell_s^2 > k^2$. Suppose that there is a layer close to the surface in which $\ell_s^2 > k^2$ and above this $\ell_s^2 < k^2$ (Fig. 10).

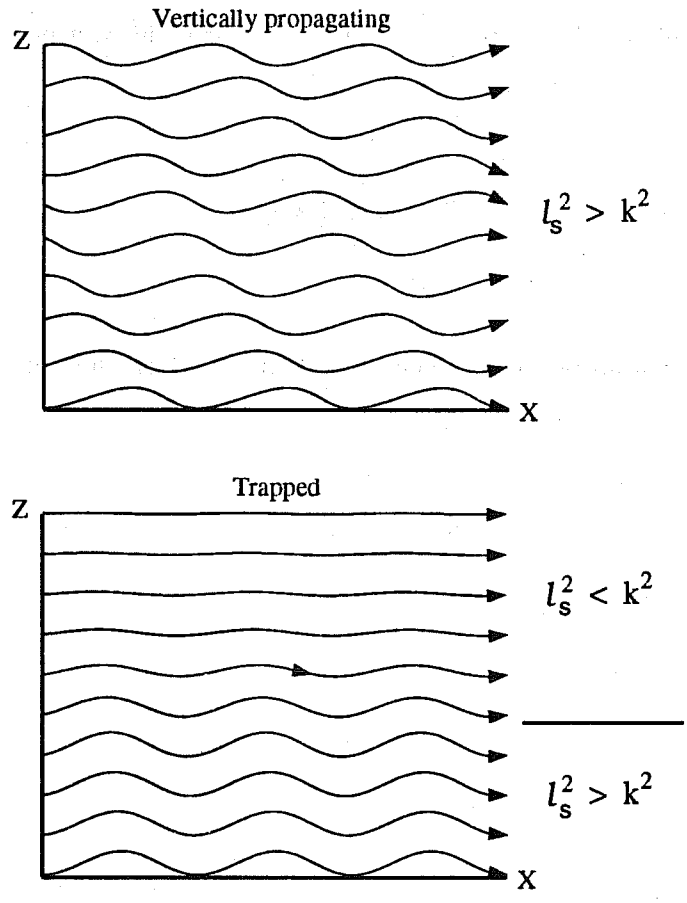

Fig. 10 Vertically propagating and trapped waves.

1. Lower layer. $\ell_s^2 > k^2$. Superimposed upward and downward (reflected) propagating waves, giving no phase slant with height.
2. Upper layer. $\ell_s^2 < k^2$. Decay of wave amplitude with height.

The wave energy is trapped in the lower layer. As there is no slant of phase lines, the wave induced stress would appear to be zero. However, there can still be a drag, because the waves extend an infinite distance downstream and there is a drag at very large distances from the orography. This is more difficult to calculate or measure than the vertically propagating case (Bretherton 1969).

9. STRONGLY STRATIFIED FLOW OVER OROGRAPHY

When the flow is strongly stratified, rather different processes occur. Consider air flowing towards a mountain at a height ζ below the summit. Can it get over the summit, or does it have to go around? Suppose that the wind speed is U and the Brunt-Väisälä frequency is N. Then the kinetic energy per unit volume of air is

$$\text{K.E.} = \frac{1}{2}\rho_0 U^2 \lambda. \tag{43}$$

If the air rises a distance ζ in order to get over the top, then at its highest point it has gained potential energy given by

$$\text{P.E.} = \frac{1}{2}\rho_0 N^2 \zeta^2. \tag{44}$$

This can only happen if the initial kinetic energy is greater than the final potential energy, i.e.

$$\frac{1}{2}\rho_0 U^2 > \frac{1}{2}\rho_0 N^2 \zeta^2 \tag{45}$$

which means that

$$\zeta < \frac{U}{N}. \tag{46}$$

Air initially at a lower level must flow *around* the mountain. The importance of stratification is measured in terms of the *Froude number* Fr given by

$$\text{Fr} = \frac{U}{NH} \tag{47}$$

where H is the mountain height. The condition for the air to be able to flow over the mountain is therefore

$$\zeta < \frac{U}{N} = \text{Fr}H. \tag{48}$$

This result is only *approximate* because it doesn't take full account of the dynamics, but it is a good guide. It also means that it is only the flow over the summit region ($< \text{Fr}H$ from the summit) which can generate internal gravity waves, because the lower flow is approximately horizontal. The main contribution to the drag therefore comes from the summit region. The qualitative picture of the flow is shown in Fig. (11).

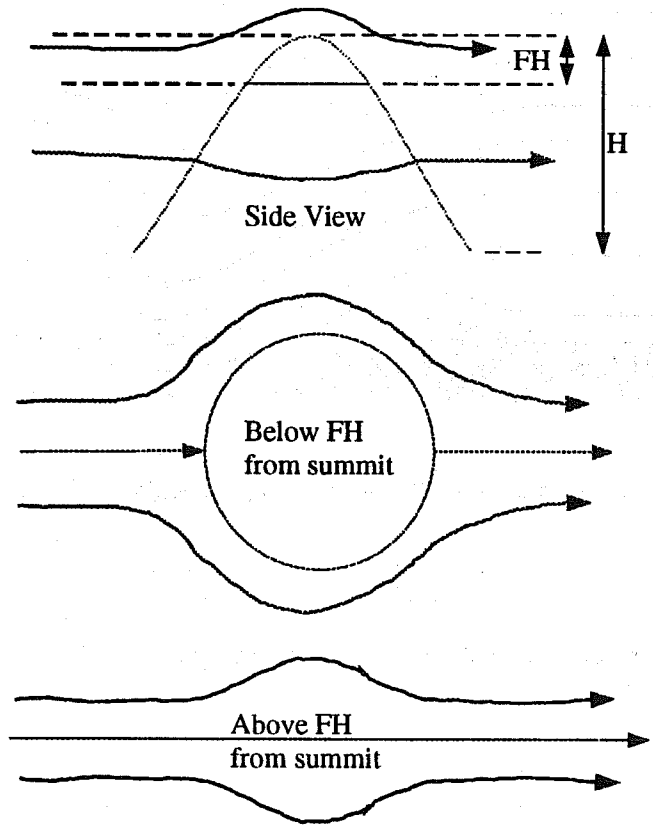

Fig. 11 Flow over and around a mountain under strongly stratified conditions.

10. BREAKING LEE WAVES AND HIGH DRAG STATES

The importance of wave breaking for wave-induced mean forcing has been emphasised in earlier sections. In §8 we also described how trapped lee waves could exert a drag force at large distances from the orography. Another phenomenon occurs when lee wave trapping is accompanied by low Froude numbers. Then the flow is highly nonlinear and lee wave breaking tends to occur directly over the orography. High drag states occur preferentially when the lee waves are trapped within a layer of thickness H, the depth of which satisfies the condition

$$H = \frac{U}{N}\left(\frac{3\pi}{2} + d + 2n\pi\right) \tag{49}$$

where D is the depth of any region of upstream blocked flow. This theory was developed by Smith (1985) and supported by numerical experiments (e.g. Bacmeister and Pierrehumbert 1988) and by laboratory experiments (e.g. Rottman and Smith 1989). In the atmosphere, the upper boundary to the trapping layer is usually a critical level. Fig. (12) shows this type of flow schematically. Note the internal hydraulic jump behaviour.

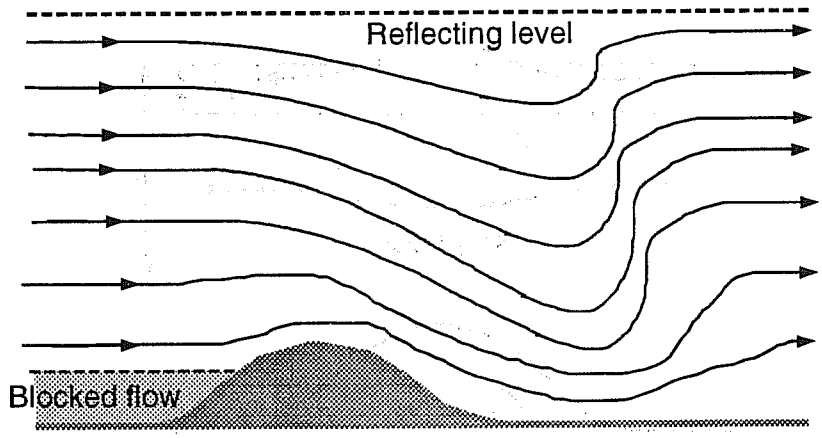

Fig. 12 Schematic illustration of the streamline pattern corresponding to a high-drag state with breaking lee waves.

11. SURFACE-BASED MEASUREMENT OF GRAVITY WAVE DRAG

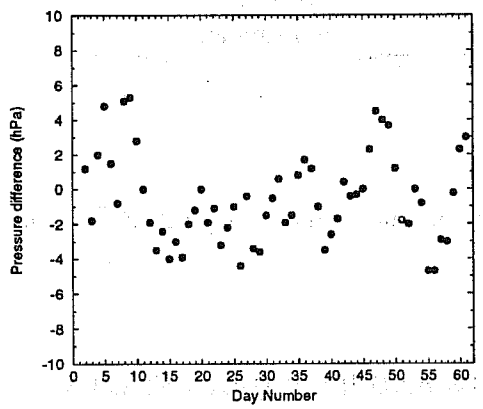

Fig. 13 Drag on the Pyrénées measured using microbarographs during a 2 month period during the PYREX experiment. The points are individual measurements of the pressure difference between stations on either side of the mountain range. (From Bougeault *et al.* 1993.)

As noted in §3, gravity wave drag observations may be based either upon observations of the waves within the free atmosphere or on measurements of the pressure force on mountains. The latter approach has been carried out on several occasions using microbarographs (e.g. Smith 1978; Richner 1987; Bougeault *et al.* 1993; Vosper 1994). The idea is to set up an array of microbarographs on a mountain or mountain range and to measure the small pressure difference between the upstream and downstream sides of the mountain. Typical pressure differences are usually less than 5 hPa and so long-term stability to better than about 0.5 hPa is required. Unless all the instruments are situated at the same height to a high degree of accuracy, the pressure differences are dominated by a hydrostatic

contribution which plays no part in the drag. This can be eliminated either by very accurate surveying or by subtracting out pressure time averages obtained from low wind conditions when the dynamical contribution to the pressure is small. Care must also be taken to eliminate the effect of the synoptic pressure gradient, if the horizontal size of the array is sufficiently large.

The interpretation of measurements can often be enhanced using detailed models of the local flow.

Examples of pressure difference and drag measurements made using microbarographs are shown in Figs. (13) and (14).

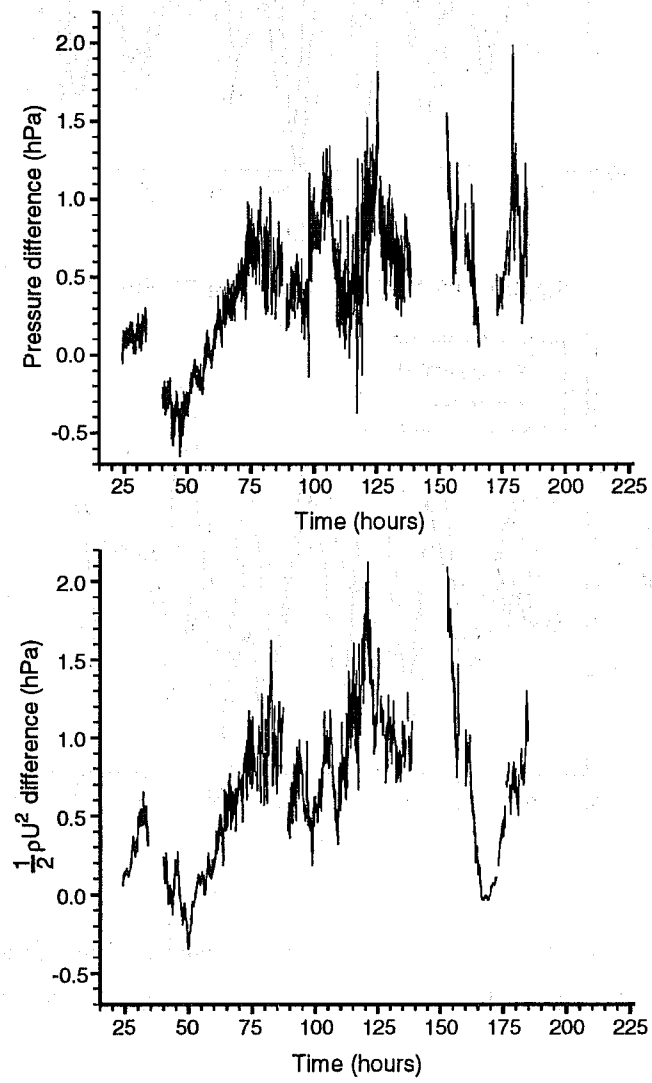

Fig. 14 Pressure difference measured across Black Combe, Cumbria, U.K. during a 10 day period, compared with the difference of $\frac{1}{2}\rho U^2$ during the same period. The close correspondence between the two measurements is a consequence of Bernoulli's equation, Eq. (6). (From Mobbs and Vosper 1994.)

12. OBSERVATIONS OF INTERNAL GRAVITY WAVES

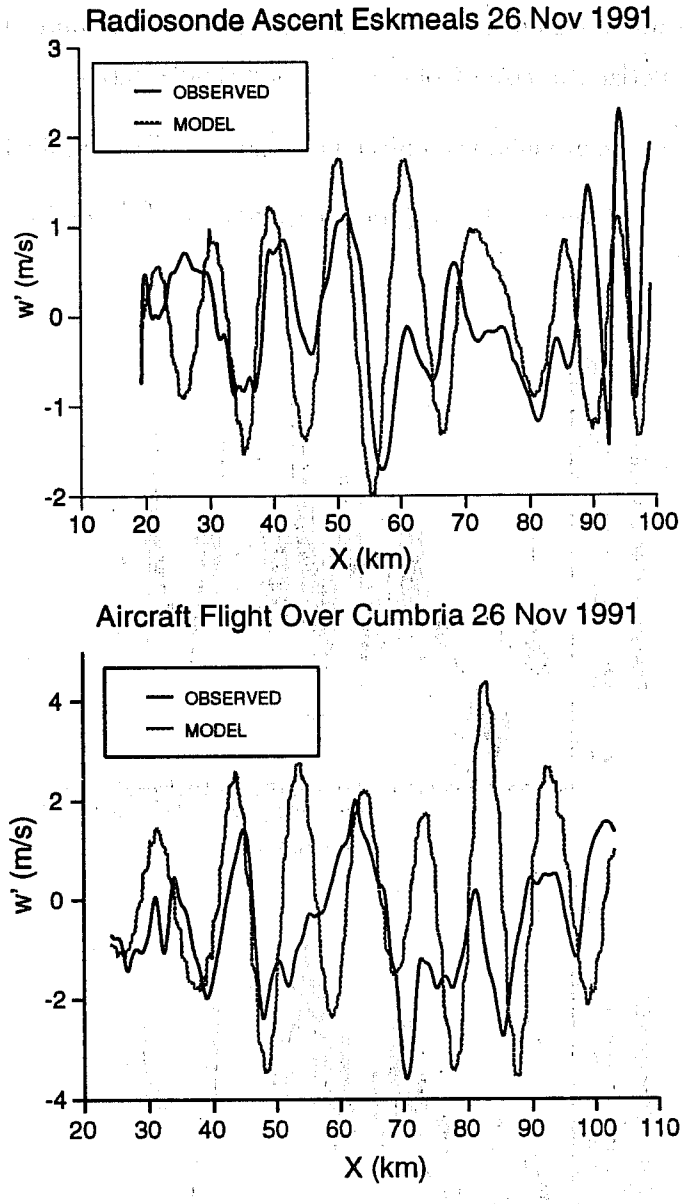

Fig. 15 The vertical velocity measured using radiosonde and aircraft over Cumbria, showing a large amplitude lee wave. Also shown for comparison are the predictions of a linear wave model (Vosper 1994).

Estimation of wave-induced stresses may be made by direct observations of the waves. There have been many such studies and they are too numerous to list here. Techniques include aircraft measurements, radiosonde measurements, radar and satellite observations. Just as with surface pressure measurements, interpretation can be enhanced using local model calculations.

Some observations of large amplitude lee waves, made using an aircraft and radiosondes, are

shown in Fig. (15). The comparison with some linear wave model computations is also shown.

13. BASIC PRINCIPLES OF GRAVITY WAVE STRESS PARAMETRIZATION

In this section we give a simplified account of some of the principles involved in parametrizing gravity wave stress in numerical weather prediction models. It is based on the parametrization suggested by Baines and Palmer (1990). Two regimes are identified, corresponding to strongly stratified flow (Fr < 1) and weakly stratified flow (Fr > 1). More precisely, the distinction between the regimes is based on an inverse Froude number $\nu = N\mu_h/U$, where μ_h is the standard deviation of the orographic height within a grid cell.

13.1 Weakly stratified flow — $\nu < 1$

We wish to parametrize the effect of the wave induced stress due to vertically propagating or trapped gravity waves and so, as we saw in §4, it is necessary to estimate $\tau_w = \rho_0 \overline{u'w'}$. From the continuity equation, Eq. (11),

$$u' = -\frac{m}{k} w'$$

and from Eq. (12)

$$ikU\widehat{\zeta} = \widehat{w}.$$

Therefore

$$|\tau| = \rho_0 |\overline{u'w'}| = \frac{\rho_0 m \overline{w'^2}}{k} = \rho_0 k |m| U^2 \overline{\zeta^2} = \frac{1}{2}\rho_0 k |m| U^2 \widehat{\zeta}^2.$$

Assuming horizontal wavelengths large compared with U/N (the hydrostatic assumption), it follows from the dispersion relation, Eq. (36), that

$$|m| = \frac{N}{U} \tag{50}$$

and hence

$$|\tau| = \frac{1}{2}\rho_0 k U N \widehat{\zeta}^2. \tag{51}$$

In practice, the stress at the surface (pressure level p_s) is a vector $\boldsymbol{\tau}_w(p_s) = (\tau_1, \tau_2)$ which is expressed in the form

$$\boldsymbol{\tau}_w = K_1 \rho_0 U N \mu_h^2 (A_1, A_2) \tag{52}$$

where K_1 is a tunable constant and A_1, A_2 are functions of the anisotropy of the orography and the angle between the surface wind vector and the principal axis of the orography.

It is necessary to know not only the surface stress but also how the stress varies with height. The height variation depends on the profiles of U and N. Consistent with the hydrostatic approximation, the theory of §8 indicates that wave trapping will occur if there is a level above which $\ell_s < 0$. The procedure to be adopted in that case is to allow the stress vector to decrease linearly to zero within

the trapping layer. If there is no trapping, then waves may encounter a critical level. If so, the stress is held constant with height up to a level close to the critical level and is then decreased rapidly to zero to represent wave absorption. The other factor which may affect the wave-induced stress is saturation. Should this occur, then the wave amplitude will be limited according to Eq. (35), so that Eq. (51) should be replaced by

$$|\tau| = \frac{1}{2}\frac{\rho_0 k U^3}{N}. \tag{53}$$

In practice, the saturation effect is represented in a more sophisticated manner. Rather than assuming that wave breakdown only occurs when isentropic surfaces become vertical, a local Richardson number is calculated and it is assumed that breakdown occurs when this falls below a critical value (usually 1/4).

13.2 Strongly stratified flow — $\nu > 1$

In this case, the flow is nonlinear. As described in §9, there is a tendency for flow at levels below U/N from the mountain tops to flow around the mountains, not over them. In a region of complex orography, this will tend to cause the flow to be around the whole region at low levels. The effect may be parametrized by adding a large drag force at levels below distance U/N below the mountain tops (which for simplicity may be assumed to be at height $2\mu_h$).

At levels above $2\mu_h - U/N$, two processes need to be represented. Firstly there will be saturated vertically propagating modes and secondly there is the possibility of high drag states associated with hydraulic flow and breaking lee waves. To represent these effects, the stress vector is written as

$$\boldsymbol{\tau} = \boldsymbol{\tau}_w + \boldsymbol{\tau}_{\mathrm{Fr}}. \tag{54}$$

The wave stress $\boldsymbol{\tau}_w$ may be represented in a similar way to that described in Eq. (53). Specifically,

$$\boldsymbol{\tau}_w(p_t) = \frac{K_2 \rho_0 U^3}{N}(A_1, A_2) \tag{55}$$

where A_1, A_2 are the same functions as in Eq. (52) and K_2 is another tuning parameter. p_t is the pressure at distance U/N below the mountain tops. The height variation of $\boldsymbol{\tau}_w$ is represented in the same way as for the $\nu < 1$ case. The hydraulic contribution $\boldsymbol{\tau}_{\mathrm{Fr}}$ is represented as follows:

$$\boldsymbol{\tau}_{\mathrm{Fr}} = \frac{K_3 \rho_0 U^3}{N}(\nu - 1)(A_1, A_2). \tag{56}$$

The factor $\nu - 1$ represents the weakening of the hydraulic effect as ν approaches 1 and the flow becomes less strongly stratified. In this case, a rather different height variation of $\boldsymbol{\tau}_{\mathrm{Fr}}$ is assumed. As noted in §10, high drag states occur for certain values of the depth H of the lee wave trapping region. These are given by Eq. (49), which may be simplified by neglecting upstream blocking and higher order trapping modes giving

$$H = \frac{3\pi}{2}\frac{U}{N}.$$

Since U and N are in fact functions of height, this may be more usefully written in the form

$$\int_0^H \frac{N}{U}\,\mathrm{d}z = \frac{3\pi}{2}. \tag{57}$$

τ_{Fr} is then allowed to decrease linearly to zero between the distance U/N below the mountain tops and height H.

14. REFERENCES

Bacmeister, J.T and Pierrehumbert, R.T.,1988: On high-drag states of nonlinear stratified flow over an obstacle. J. Atmos. Sci., **45**, 63–80.

Baines, P.G. and Palmer, T.N., 1990: Rationale for a new physically-based parametrization of subgridscale orographic effects. ECMWF Technical Memorandum No. 169.

Bougeault, P., Jansa, A., Attie, J.L., Beau, L., Benech, B., Benoit, R., Bessemoulin, P., Caccia, J.L., Campins, J., Carissimo, B., Champeaux, J.L., Crochet, M., Druilhet, A., Durand, P., Elkhalfi, A., Flamant, P. Genoves, A., Georgelin, M., Hoinka, K.P., Klaus, V., Koffi, E., Kotroni, V., Mazaudier, C. Pelon, J., Petitdidier, M., Pointin, Y. Puech, D., Richard, E., Satomura, T., Stein, J. and Tannhauser, D., 1993: The atmospheric momentum budget over a major mountain range: first results of the PYREX field program. *Ann. Geophysicae*, **11**, 395–418.

Bretherton, F.P., 1969: Momentum transport by gravity waves. *Quart. J. R. Met. Soc.*, **95**, 213–243.

Bretherton, F.P. and Garrett, C.J.R., 1968: Wave trains in inhomogeneous moving media. *Proc. Roy. Soc. Lond.*, **A302**, 529–554.

Eliassen, A. and Palm, E., 1961: On the transfer of energy in stationary mountain waves, *Geofys. Publ.*, **22**, 1–23.

Lindzen, R.S., 1981: Turbulence and stress due to gravity wave and tidal breakdown. *J. Geophys. Res.*, **86**, 9707–9714.

Mobbs, S.D. and Vosper, S.B., 1994: Measurement of the pressure force on a hill, in preparation.

Palmer, T.N., Shutts, G.J. and Swinbank, R., 1986: Alleviation of a systematic westerly bias in general circulation and numerical weather prediction models through an orographic gravity wave parametrization. *Quart. J. R. Met. Soc.*, **112**, 1001–1039.

Richner, H., 1987: The design and operation of a microbarograph array to measure pressure drag on the mesoscale. *J. Atmos. Oceanic Technol.*, 4, 105–112.

Rottman, J.W. and Smith, R.B., 1989: A laboratory model of severe downslope winds. *Tellus*, **41A**, 401–415.

Smith, R.B., 1978: A measurement of mountain drag. *J. Atmos. Sci.*, **35**, 1644–1654.

Smith, R.B., 1985: On severe downslope winds. *J. Atmos. Sci.*, **42**, 2597–2603.

Vosper, S.B., 1994: *Observations and modelling of orographic internal gravity waves*, Ph.D. thesis, University of Leeds.

APPENDIX. DERIVATION OF THE ELIASSEN-PALM THEOREM

The linearised momentum equations (2-D here, but it works in 3-D) are:

$$\rho_0 U\frac{\partial u'}{\partial x}+\rho_0\frac{\mathrm{d}U}{\mathrm{d}z}w'=-\frac{\partial p'}{\partial x}; \tag{A1}$$

$$\rho_0 U\frac{\partial w'}{\partial x}=-\frac{\partial p'}{\partial z}+\rho_0 g\frac{\theta'}{\theta_0}; \tag{A2}$$

$$U\frac{\partial\theta'}{\partial x}+w'\frac{\mathrm{d}\bar{\theta}}{\mathrm{d}z}=0; \tag{A3}$$

$$\frac{\partial u'}{\partial x}+\frac{\partial w'}{\partial z}=0. \tag{A4}$$

We can form wave energy equation from Eq. (1) $\times\, u'$ + Eq. (2) $\times\, w'$

$$\frac{\partial}{\partial x}\left[\frac{\rho_0 U}{2}(u'^2+w'^2)+p'u'\right]+\frac{\partial}{\partial z}(p'w')-\frac{\rho_0 g}{\theta_0}w'\theta'=-\rho_0\frac{\mathrm{d}U}{\mathrm{d}z}u'w'.$$

From Eq. (A3) and

$$U\frac{\partial\zeta}{\partial x}=w' \tag{A5}$$

it follows that

$$U\frac{\partial\theta'}{\partial x}+U\frac{\partial\zeta}{\partial x}\frac{\mathrm{d}\bar{\theta}}{\mathrm{d}z}=0.$$

If $U\neq 0$ it follows that

$$\theta'=-\zeta\frac{\mathrm{d}\bar{\theta}}{\mathrm{d}z}.$$

The wave energy equation becomes

$$\frac{\partial}{\partial x}\left[\frac{\rho_0 U}{2}(u'^2+w'^2+N^2\zeta^2)+p'u'\right]+\frac{\partial}{\partial z}(p'w')=-\rho_0\frac{\mathrm{d}U}{\mathrm{d}z}u'w'.$$

This equation can be averaged horizontally if the waves decay at $\pm\infty$ (this excludes perfectly trapped lee waves) giving

$$\frac{\partial}{\partial z}(\overline{p'w'})=-\rho_0\frac{\mathrm{d}U}{\mathrm{d}z}\overline{u'w'}. \tag{A6}$$

This equation reveals a significant result:

The vertical flux of wave energy varies with height when there is shear.

Now take Eq. (1) $\times\, (\rho_0 U u'+p')$:

$$\frac{\partial}{\partial x}\left[\frac{\rho_0^2U^2}{2}u'^2+\rho_0 U p'u'+\frac{p'}{2}\right]+\rho_0^2 U\frac{\mathrm{d}U}{\mathrm{d}z}u'w'.+\rho_0\frac{\mathrm{d}U}{\mathrm{d}z}p'w'=0$$

averaging this horizontally

$$\rho_0 U\overline{u'w'}=-\overline{p'w'}. \tag{A7}$$

Hence, from Eq. (A6) and Eq. (A7)

$$\frac{\partial}{\partial z}(\rho_0 U\overline{u'w'})=\rho_0\overline{u'w'}\frac{\mathrm{d}U}{\mathrm{d}z}$$

which implies that

$$\frac{\partial}{\partial z}(\rho_0\overline{u'w'})=0\quad\text{except where } U=0.$$

This means that the vertical flux of horizontal momentum is independent of height except near levels where $U=0$. These are *critical levels.*